Inverse Problems 11 (1995) 1225–1232. Printed in the UK

A propagation–backpropagation method for ultrasound tomography

Frank Natterer and Frank Wübbeling

Institut für Numerische und instrumentelle Mathematik, Universität Münster, Einsteinstrasse 62, D-48149 Münster, Germany

Received 20 June 1995

Abstract. Ultrasound tomography is modelled by the inverse problem of a 2D Helmholtz equation at fixed frequency with plane-wave irradiation. It is assumed that the field is measured outside the support of the unknown potential f for finitely many incident waves. Starting out from an initial guess f^0 for f we propagate the measured field through the object f^0 to yield a computed field whose difference to the measurements is in turn backpropagated. The backpropagated field is used to update f^0. The propagation as well as the backpropagation are done by a finite difference marching scheme. The whole process is carried out in a single-step fashion, i.e. the updating is done immediately after backpropagating a single wave. It is very similar to the well known ART method in X-ray tomography, with the projection and backprojection step replaced by propagation and backpropagation.

1. Description of the method

We consider the following inverse problem for the Helmholtz equation. Find the potential f from

$$\Delta u_\theta + k^2(1-f)u_\theta = 0 \qquad u_\theta(x) = e^{ikx\cdot\theta}(1+v_\theta) \tag{1.1}$$

where $e^{ikx\cdot\theta}v_\theta$ satisfies the Sommerfeld radiation condition. The positive number k is fixed, and θ runs through all unit vectors in $\mathbb{R}^2$. It is assumed that $f = 0$ and $v_\theta = g_\theta$ outside $\Omega = \{x = |x| < \rho\}$ with g_θ a given function. In fact, it suffices to know g on a circle containing Ω.

The uniqueness has recently been settled by Nachman [9]. In this paper we give a numerical algorithm which computes an approximation to f from finitely many directions $\theta_0, \ldots, \theta_{p-1}$. Most of the existing algorithms use the Born or Rytov approximation (diffraction tomography). The algorithms of diffraction tomography are of the filtered backpropagation type (Devaney [3]) or simply inverse Fourier transforms, see Kak and Slaney [6]. Methods which avoid the Born and Rytov approximation have been given, e.g. by Borup *et al* [1], Kleinman and van den Berg [7], Colton and Monk [2] and Gutman and Klibanov [5]. These algorithms are iterative in nature. They suffer from excessive computing times and from their apparent inability to handle problems with large values of k. A novel approach which has yet to be tested numerically has been suggested by Stenger and O'Reilly [13].

The method of the present paper is iterative, too. It differs from existing ones in two respects. First, we avoid the computation of large Jacobians by considering only one wave at a time, solving a vastly underdetermined problem with the help of an

0266-5611/95/061225+08$19.50

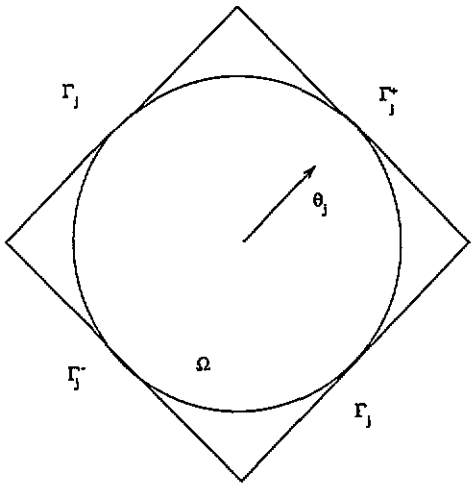

Figure 1. Basic geometry. Q_j is the square of side length 2ρ whose boundary is made up of Γ_j, Γ_j^- and Γ_j^+.

approximate generalized inverse. This generalized inverse can be computed very efficiently by backpropagation. Second, we make use of a novel and highly efficient finite difference method for doing the propagation step. It is essentially a method for solving the Cauchy problem for the Helmholtz equation. Contrary to general belief, this problem is perfectly stable as long as only spatial frequencies below k are sought for. Since we do not expect to be able to determine frequencies larger than k, this restriction is quite natural.

On a more formal level, our algorithm is as follows. Consider a square Q_j circumscribed to Ω with two edges Γ_j parallel to θ_j and with edges Γ_j^+, Γ_j^- orthogonal to θ_j, with Γ_j^+ lying in the direction of θ_j, see figure 1. Let R_j: $L_2(Q_j) \to L_2(\Gamma_j^+)$ be the (nonlinear) operator which associates with each potential $f \in L_2(\Omega)$ the solution $v_j = v_{\theta_j}$ of (1.1) on Γ_j^+, the values of v_j on $\Gamma_j \cup \Gamma_j^-$ and the values of $\frac{\partial}{\partial \nu} v_j$ (ν the interior normal on ∂Q_j) on Γ_j^- being given by the data function g_{θ_j}. Thus, if v_j is the solution to

$$\begin{aligned} &\Delta v_j + 2ik\theta_j \cdot \nabla v_j - k^2 v_j f = k^2 f \qquad \text{in} \quad Q_j \\ &v_j = g_{\theta_j} \qquad \text{on} \quad \Gamma_j \cup \Gamma_j^- \qquad \frac{\partial}{\partial \nu} v_j = \frac{\partial}{\partial \nu} g_{\theta_j} \qquad \text{on} \quad \Gamma_j^- \end{aligned} \tag{1.2}$$

then $R_j f = v_j$ on Γ_j^+. With g_j the function g_{θ_j} restricted to Γ_j^+, we have

$$R_j(f) = g_j \qquad j = 0, \ldots, p-1\,. \tag{1.3}$$

This nonlinear system is solved for f in the following way. Let f^0 be an initial approximation. Once f^r is determined, put $f^{r+1} = f^r + \omega d^r$ where d^r is an approximation to the minimal norm solution of

$$R_j(d^r + f^r) = g_j \qquad j = r \bmod p \tag{1.4}$$

where ω is a relaxation factor. Thus our algorithm is simply a nonlinear version of the Kaczmarz method which has become known as ART (algebraic reconstruction technique) in x-ray tomography, see Herman [4], Natterer [10]. As in ART, we call the successive computation of p iterates a complete sweep.

For the approximate solution of (1.4) we linearize (1.3), writing

$$R_j(d + f) = R_j(f) + A_j(f)d + O(d^2)\,.$$

Here, $A_j(f) : L_2(\Omega) \to L_2(\Gamma_j^+)$ is the linear operator defined by solving

$$\begin{aligned} &\Delta w + 2ik\theta_j \cdot \nabla w - k^2 wf - k^2(1+v_j)d = 0 \qquad \text{in} \quad Q_j \\ &w = 0 \qquad \text{on} \quad \Gamma_j \cup \Gamma_j^- \qquad \frac{\partial w}{\partial \nu} = 0 \qquad \text{on} \quad \Gamma_j^- \end{aligned} \tag{1.5}$$

and v_j is the solution of (1.2), and putting $A_j(f)d$ equal to the restriction of w to Γ_j^+.

In [11] we used a simpler version of $A_j(f)$, omitting the term $k^2 wf$ in (1.5). Meanwhile numerical experiments showed that the gain in simplicity thus obtained does not make up for the loss in accuracy.

In order to compute an approximate minimal norm solution d^r in (1.4) we make use of the adjoint operator $A_j^*(f) : L_2(\Gamma_j^+) \to L_2(Q_j)$. For $g \in L_2(\Gamma_j^+)$ this operator can be evaluated by solving

$$\begin{aligned} &\Delta z + 2ik\theta_j \cdot \nabla z - k^2 \overline{f} z = 0 \qquad \text{in} \quad Q_j \\ &z = 0 \qquad \text{on} \quad \Gamma_j \cup \Gamma_j^+ \qquad \frac{\partial z}{\partial \nu} = g \qquad \text{on} \quad \Gamma_j^+ \end{aligned} \tag{1.6}$$

for z and putting

$$A_j^*(f)g = k^2(1+\overline{v}_j)z \tag{1.7}$$

with v_j from (1.2). In fact, for sufficiently smooth functions w, z, Green's formula and an integration by parts show that

$$\int_{Q_j} \left\{ (\Delta w + 2ik\theta_j \cdot \nabla w - k^2 f w)\overline{z} - w\overline{(\Delta z + 2ik\theta_j \cdot \nabla z - k^2 \overline{f} z)} \right\} \mathrm{d}x$$

$$= \int_{\partial Q_j} \left(w \frac{\partial \overline{z}}{\partial \nu} - \frac{\partial w}{\partial \nu} \overline{z} \right) \mathrm{d}s + 2ik \left(\int_{\Gamma_j^+} w\overline{z}\, \mathrm{d}s - \int_{\Gamma_j^-} w\overline{z}\, \mathrm{d}s \right)$$

where ν is the interior normal and s the arc length on ∂Q_j. Applying this to w from (1.5) and z from (1.6) yields

$$k^2 \int_{Q_j} d(1+v_j)\overline{z}\, \mathrm{d}x = \int_{\Gamma_j^+} w\overline{g}\, \mathrm{d}s$$

or

$$k^2 (d, (1+\overline{v}_j)z)_{L_2(Q_j)} = (A_j(f)d, g)_{L_2(\Gamma_j^+)}$$

hence equation (1.7).

We now define d^r to be

$$d^r = A_j(f^r)^* C_j (R_j(f^r) - g_j) \tag{1.8}$$

with some operator C_j. If $C_j = (A_j(f^r)A_j(f^r)^*)^{-1}$, then d^r is the minimum norm solution of the linearized system. Since the computation of this operator is very time consuming we simply replace it by its value for large k, namely $C_j = \rho k^{-2} I$. We found that this choice of C_j yields good convergence to the solution of the fully nonlinear problem.

This describes our algorithm apart from discretization and filtering which are discussed later. The algorithm consists of the propagation step, in which the measured field is propagated from Γ_j^- to Γ_j^+, assuming f^r to be the potential, to yield the function $R_j(f^r)$ on Γ_j^+. Then the function $g = R_j(f^r) - g_j$ is backpropagated from Γ_j^+ to Q_j by solving the initial-value problem (1.6). Finally, the backpropagated field is used to update f^r.

We call $A_j(f^r)^*$ the backpropagation operator and the whole method the propagation–backpropagation algorithm (PBP).

The similarity of PBP to the ART algorithm of computerized tomography is obvious. The propagation and backpropagation step of PBP corresponds to the projection and backprojection step, respectively of ART. It seems that much of the well understood theory of ART (see, for example, Natterer [10]) also applies to PBP. For instance, reordering of the equations (1.3) has a decisive influence on the behaviour of the iterates.

2. Discretization and filtering

The implementation of PBP is very easy. All we need are subroutines for the initial-value problems (1.2) and (1.6). In [12, 14] it is shown how to solve these initial-value problems in a stable way by a straightforward finite difference method. A similar method has been suggested by Knightly and Mary [8]. We give the details only for (1.2).

In Q_j we introduce the grid $Q_j^h = \{x_{\ell,m} = h\ell\theta_j + hm\theta_j^\perp\colon \ell, m = -q, \dots, q\}$, $h = 1/q$. On Q_j^h we define the approximation $v_{\ell,m}$ to $v_j(x_{\ell,m})$ by

$$\begin{aligned} &v_{\ell+1,m} + v_{\ell-1,m} + v_{\ell,m-1} + v_{\ell,m+1} - 4v_{\ell,m} \\ &\qquad + \mathrm{i}\varepsilon(v_{\ell+1,m} - v_{\ell-1,m}) - \varepsilon^2(1 + v_{\ell,m})f(x_{\ell,m})v_{\ell,m} = 0 \\ &\qquad |\ell| < q \qquad |m| < q \qquad \varepsilon = hk\,. \end{aligned} \tag{2.1}$$

These equations are complemented by the boundary conditions

$$v_{\ell,m} = g_{\theta_j}(x_{\ell,m}) \qquad \text{for} \quad |m| = q, \quad |\ell| \leqslant q$$

and by the initial conditions

$$\begin{aligned} &v_{-q,m} = g_{\theta_j}(x_{\ell,m}) \qquad |m| \leqslant q \\ &v_{1-q,m} = h(1 - \mathrm{i}\varepsilon)\frac{\partial}{\partial v} g_{\theta_j}(x_{-q,m}) - \tfrac{1}{2} g_{\theta_j}(x_{-q,m+1}) - \tfrac{1}{2} g_{\theta_j}(x_{-q,m-1}) + 2g_{\theta_j}(x_{-q,m}) \\ &\qquad |m| < q\,. \end{aligned}$$

The latter expression has been derived by using central differences in the discretization of $\partial/\partial v$ and (2.1) for $\ell = -q$.

Equation (2.1) can be solved recursively for $v_{\ell+1,m}$, $\ell = -q+1, \dots, q-1$, yielding the approximation $v_{q,m}$ to $R_j f(x_{q,m})$, $|m| \leqslant q$. According to [12], the recursion is stable if $h \geqslant \pi/k\sqrt{1-f}$. If a smaller stepsize is chosen, stability can be restored by filtering the vector $v_{\ell,m}$ as a function of m after each step $\ell \to \ell + 1$. This can be done by the discrete Fourier transform. Putting

$$\hat{v}_{\ell,n} = \frac{1}{2q} \sum_{m=-q}^{q-1} \mathrm{e}^{-\mathrm{i}mn\pi/q} v_{\ell,m}$$

the filtered version of $v_{\ell,m}$ is

$$v'_{\ell,m} = \sum_{|n| \leqslant N} \mathrm{e}^{+\mathrm{i}mn\pi/q} \hat{v}_{\ell,n}$$

where $N \leqslant \frac{\varrho}{\pi} k\sqrt{1-f}$. The filtering can be done by the fast Fourier transform (FFT). For details see [12, 14]. After each complete sweep of the algorithm we perform a 2D filtering of the current approximation which annihilates frequency components $> k$ which come in during the iteration.

The number of operations one needs for each initial-value problem is q^2 or $q^2 \log q$ if filtering is used. For a whole sweep of PBP $2p$ initial-value problems have to be solved.

Thus a complete sweep needs pq^2 or $pq^2 \log q$ operations. Apart from the logarithm this is the complexity of one complete sweep of the ART algorithm in x-ray tomography. Thus PBP does ultrasound tomography with almost the same speed as ART does x-ray tomography.

3. Numerical experiments

In a first experiment we reconstructed the rotationally symmetric function

$$f(x) = \begin{cases} 0.1 & |x| \leqslant 0.8 \\ 0 & \text{otherwise} \end{cases} \tag{3.1}$$

for $k = 50$ from $p = 100$ directions. The scattered waves can be computed exactly for this potential. Thus we have exact data. The reconstruction region is the square of side length 2 with the midpoint at the origin. The reconstruction is done on a 129×129 grid.

This example has been chosen in such a way that the Born approximation, which is the basis of difraction tomography, is not valid. The condition for the Born approximation to hold is (for real potentials)

$$|Rf| \ll \frac{2\pi}{k} \tag{3.2}$$

where R is the Radon transform (i.e. Rf stands for the set of all line integrals of f). This is a slight extension of the condition given in [6], p 214. In our case we have

$$|Rf| \leqslant 0.160 \qquad \frac{2\pi}{k} = 0.126$$

hence equation (3.2) is not satisfied.

We did the reconstruction with $f^0 = \frac{1}{2} f$ and $\omega = 1$. The choice of f^0 is such that

$$|R(f - f^0)| \leqslant \frac{2\pi}{k}. \tag{3.3}$$

Thus, while the Born approximation is not valid for f, it does hold for $f - f^0$. This condition for the initial approximation seems to be necessary for convergence, see [14] for a discussion.

The results after three sweeps are displayed in figure 2. The reconstructed potential differs from the exact potential in the interior by only 3%, but at the boundary a loss in resolution is noticeable. However, one has to bear in mind that the wavelength $\lambda = 2\pi/k$ of the irradiating wave is 0.126, which sets a limit to the achievable spatial resolution.

In a second numerical test we created an elliptical phantom, see figure 3. On an elliptical base of density 0.15 sits—slightly misalligned—a smaller ellipse with semi axes 0.8, 0.6 and density 0.2, which contains two circles with density 0.21, 0.19, respectively, and a square with side length 0.12 and density 0.25. So far the real part of the potential. The imaginary part is 0.02 in the base and zero elsewhere. The size of the square corresponds to the wavelength $\lambda = 2\pi/k$, $k = 50$, of the irradiating wave. Thus the square serves as a test for the spatial resolution, while the two circles serve as a test for the density resolution.

The PBP reconstruction after three sweeps with $\omega = 1$ is shown in figure 3. The elliptical base has been used as f^0. We see that the spatial resolution is exactly as expected, and the density resolution is better than 5%. The cross section of the reconstruction may look disappointing to someone who is used to look at CT pictures with the same amount of data. But, in fact, the reconstructed cross section in figure 3 is virtually indistinguishable from the corresponding cross section of the low-pass filtered elliptical phantom, the cut-off being put at $k = 50$.

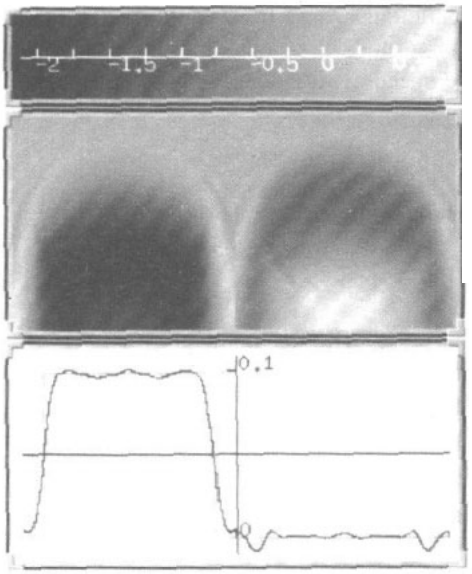

Figure 2. Reconstruction of potential (3.1) from exact data for wavenumber $k = 50$ and $p = 100$ directions. Top: scattered field $v_\theta e^{-ikx\cdot\theta}$ for the incident wave coming from the top. Real part left, imaginary part right. Backscatter is clearly visible. Bottom: cross section through original and reconstruction.

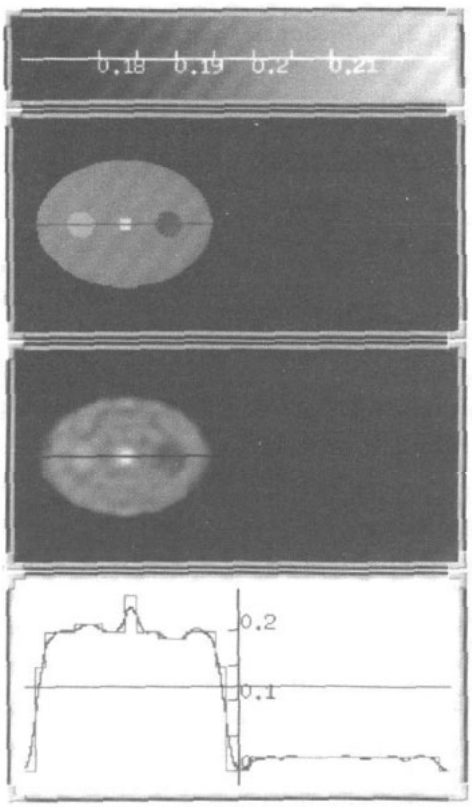

Figure 3. Reconstruction of elliptical phantom. Values of k, p as in figure 2. Top: original. Middle: PBP reconstruction after three complete sweeps. Bottom: cross section through original and reconstruction.

We computed the data by our forward solver. This is usually considered as 'inverse crime'. But we repeated the calculation after having added 5% white noise to the data—

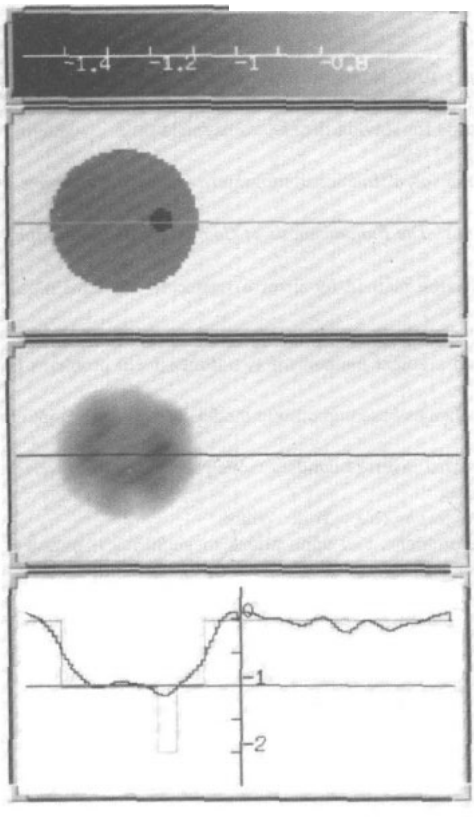

Figure 4. Reconstruction of 'finger' with $k = 7$ and 53 waves. *Top: original. Middle:* PBP *reconstruction* after three sweeps. Bottom: cross section through original and reconstruction.

without much change in the reconstruction. The computations took only a few minutes on a SUN workstation Sparc Station SS20.

For a third numerical test we chose the 'finger' from [2]. In our notation,

$$f(x) = \begin{cases} -2 & |x - x_0| \leqslant 0.1 \\ -1 & |x| < \frac{2}{3} \quad \text{and} \quad |x - x_0| > \frac{1}{3} \\ 0 & \text{otherwise} \end{cases}$$

where $x_0 = (\frac{1}{3}, 0)^T$, see figure 4. As in [2] we chose $k = 7$ and used $p = 53$ waves, and we work on a 65×65 grid. The result of PBP after three complete sweeps, again with $\omega = 1$, is displayed in figure 4. As in [2] we used $f^0 = -0.5$ as an initial approximation. This example shows that PBP can well recover details below the resolution limit of $2\pi/k = 0.90$, even though it has not been designed to do so. Of course, in order to achieve this, one has to drop the filtering after each sweep which has been mentioned in section 2.

All these examples have been done with a random ordering of the directions. This has been suggested by our experience with ART, see [10], p 165.

To conclude, PBP is a simple and very efficient algorithm. Efficiency is achieved by avoiding the computation of Jacobians and by using a marching scheme as forward solver. Of course this forward solver can be replaced by any other efficient Helmholtz solver.

References

[1] Borup D T, Johnson S A, Kim W W and Berggren M J 1992 Nonperturbative diffraction tomography via Gauss–Newton iteration applied to the scattering integral equation *Ultrasonic Imaging* **14** 69–85

[2] Colton D and Monk P 1994 A modified dual space method for solving the electromagnetic inverse scattering problem for an infinite cylinder *Inverse Problems* **10** 87–108

[3] Devaney A J 1982 A filtered backpropagation algorithm for diffraction tomography *Ultrasonic Imaging* **4** 336–50

[4] Herman G T 1980 *Image Reconstruction from Projections: The Fundamentals of Computerized Tomography* (New York: Academic)

[5] Gutman S and Klibanov M 1993 Regularized quasi-Newton method for inverse scattering problems *Math. Comput. Modelling* **18** 5–31 (Oxford: Pergamon)

[6] Kak A C and Slaney M 1987 *Principles of Computerized Tomographic Imaging* (New York: IEEE)

[7] Kleinman R E and van den Berg P M 1992 A modified gradient method for two-dimensional problems in tomography *J. Comput. Appl. Math.* **42** 17–35

[8] Knightly G H and Mary D F St 1993 Stable marching schemes based on elliptic models of wave propagation *J. Acoust. Soc. Am.* **93** 1866–72

[9] Nachman A I 1993 Global uniqueness for a two-dimensional inverse boundary value problem *Preprint series* **19** Department of Mathematics University of Rochester

[10] Natterer F 1986 *The Mathematics of Computerized Tomography* (New York: Wiley)

[11] Natterer F 1995 Finite difference methods for inverse problems and applications to geophysics, industry, medicine and technology *Proc. Int. Workshop on Inverse Problems (HoChiMinh City) Publications of The HoChiMinh City Mathematical Society* **2**

[12] Natterer F and Wübbeling F 1993 A finite difference method for the inverse scattering problem at fixed frequency *Lecture Notes in Physics* vol 422 (Berlin: Springer) p 157–66

[13] Stenger F and O'Reilly M 1994 Sinc inversion of the Helmholtz equation without computing the forward solution *Preprint* Department of Computer Science, University of Utah

[14] Wübbeling F 1994 Direktes und inverses streuproblem bei fester frequenz *Thesis* Fachbereich Mathematik, Universität Münster